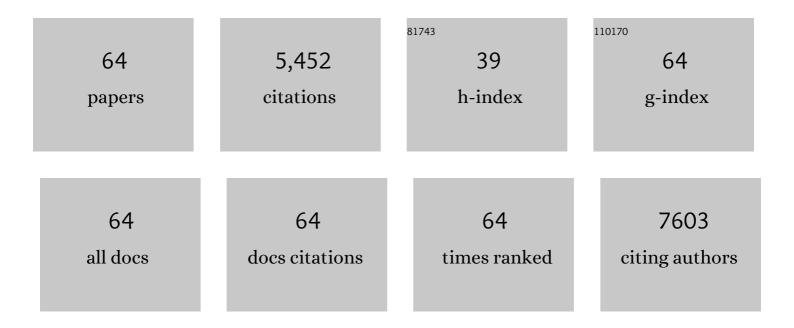
List of Publications by Year in descending order

Source: https://exaly.com/author-pdf/728787/publications.pdf Version: 2024-02-01



#	Article	IF	CITATIONS
1	Bi4TaO8Cl/Bi heterojunction enables high-selectivity photothermal catalytic conversion of CO2-H2O flow to liquid alcohol. Chemical Engineering Journal, 2022, 435, 135133.	6.6	27
2	Photothermal synergic enhancement of direct Z-scheme behavior of Bi4TaO8Cl/W18O49 heterostructure for CO2 reduction. Applied Catalysis B: Environmental, 2020, 268, 118401.	10.8	115
3	Thermal coupled photoconductivity as a tool to understand the photothermal catalytic reduction of CO2. Chinese Journal of Catalysis, 2020, 41, 154-160.	6.9	59
4	Photoreduced nanocomposites of graphene oxide/N-doped carbon dots toward all-carbon memristive synapses. NPG Asia Materials, 2020, 12, .	3.8	47
5	Anatase/Bronze TiO2 Heterojunction: Enhanced Photocatalysis and Prospect in Photothermal Catalysis. Chemical Research in Chinese Universities, 2020, 36, 992-999.	1.3	26
6	W-Doped TiO ₂ for photothermocatalytic CO ₂ reduction. Nanoscale, 2020, 12, 17245-17252.	2.8	37
7	Elucidation of the electron energy structure of TiO ₂ (B) and anatase photocatalysts through analysis of electron trap density. RSC Advances, 2020, 10, 18496-18501.	1.7	11
8	Solution plasma boosts facet-dependent photoactivity of decahedral BiVO4. Chemical Engineering Journal, 2020, 397, 125381.	6.6	28
9	Enhanced Solar Photothermal Catalysis over Solution Plasma Activated TiO ₂ . Advanced Science, 2020, 7, 2000204.	5.6	89
10	High-humidity tolerance of porous TiO2(B) microspheres in photothermal catalytic removal of NO. Chinese Journal of Catalysis, 2020, 41, 1622-1632.	6.9	14
11	Revisiting Pt/TiO ₂ photocatalysts for thermally assisted photocatalytic reduction of CO ₂ . Nanoscale, 2020, 12, 7000-7010.	2.8	73
12	Revisiting cocatalyst/TiO2 photocatalyst in blue light photothermalcatalysis. Catalysis Today, 2019, 335, 286-293.	2.2	16
13	TiO2-x/CoOx photocatalyst sparkles in photothermocatalytic reduction of CO2 with H2O steam. Applied Catalysis B: Environmental, 2019, 243, 760-770.	10.8	132
14	Ti3+ defect mediated g-C3N4/TiO2 Z-scheme system for enhanced photocatalytic redox performance. Applied Surface Science, 2018, 448, 288-296.	3.1	89
15	Control over energy level match in Keggin polyoxometallate-TiO2 microspheres for multielectron photocatalytic reactions. Applied Catalysis B: Environmental, 2018, 234, 79-89.	10.8	46
16	Minimization of defects in Nb-doped TiO 2 photocatalysts by molten salt flux. Ceramics International, 2018, 44, 10249-10257.	2.3	8
17	The W@WO ₃ ohmic contact induces a high-efficiency photooxidation performance. Dalton Transactions, 2017, 46, 1487-1494.	1.6	18
18	Transparent Nb-doped TiO ₂ films with the [001] preferred orientation for efficient photocatalytic oxidation performance. Dalton Transactions, 2017, 46, 15363-15372.	1.6	13

#	Article	IF	CITATIONS
19	Surface oxygen vacancies on WO3 contributed to enhanced photothermo-synergistic effect. Applied Surface Science, 2017, 391, 654-661.	3.1	85
20	Synergistic effect of surface self-doping and Fe species-grafting for enhanced photocatalytic activity of TiO2 under visible-light. Applied Surface Science, 2017, 396, 26-35.	3.1	28
21	Synergic effects of Cu O electron transfer co-catalyst and valence band edge control over TiO2 for efficient visible-light photocatalysis. Chinese Journal of Catalysis, 2017, 38, 2120-2131.	6.9	30
22	Enhanced photoelectrochemical performance of nanoporous BiVO4 photoanode by combining surface deposited cobalt-phosphate with hydrogenation treatment. Electrochimica Acta, 2016, 195, 51-58.	2.6	66
23	Ultrasonic spray pyrolysis assembly of a TiO2–WO3–Pt multi-heterojunction microsphere photocatalyst using highly crystalline WO3 nanosheets: less is better. New Journal of Chemistry, 2016, 40, 3225-3232.	1.4	8
24	Defect-Induced Yellow Color in Nb-Doped TiO ₂ and Its Impact on Visible-Light Photocatalysis. Journal of Physical Chemistry C, 2015, 119, 16623-16632.	1.5	142
25	Efficiency enhanced rutile TiO2 nanowire solar cells based on an Sb2S3 absorber and a Cul hole conductor. New Journal of Chemistry, 2015, 39, 7243-7250.	1.4	7
26	Correlation between band alignment and enhanced photocatalysis: a case study with anatase/TiO ₂ (B) nanotube heterojunction. Dalton Transactions, 2015, 44, 13331-13339.	1.6	29
27	Simple Ethanol Impregnation Treatment Can Enhance Photocatalytic Activity of TiO ₂ Nanoparticles under Visible-Light Irradiation. ACS Applied Materials & Interfaces, 2015, 7, 7752-7758.	4.0	78
28	Bilayer TiO ₂ photoanode consisting of a nanowire–nanoparticle bottom layer and a spherical voids scattering layer for dye-sensitized solar cells. New Journal of Chemistry, 2015, 39, 4845-4851.	1.4	23
29	Promotion of multi-electron transfer for enhanced photocatalysis: A review focused on oxygen reduction reaction. Applied Surface Science, 2015, 358, 28-45.	3.1	115
30	Vacuum heat treated titanate nanotubes for visible-light photocatalysis. New Journal of Chemistry, 2015, 39, 1281-1286.	1.4	9
31	Photoelectrochemical Water Splitting with Rutile TiO2 Nanowires Array: Synergistic Effect of Hydrogen Treatment and Surface Modification with Anatase Nanoparticles. Electrochimica Acta, 2014, 130, 290-295.	2.6	84
32	TiO2 (B) nanosheets mediate phase selective synthesis of TiO2 nanostructured photocatalyst. Applied Surface Science, 2014, 292, 937-943.	3.1	14
33	Photocatalytic activities of heterostructured TiO2-graphene porous microspheres prepared by ultrasonic spray pyrolysis. Journal of Alloys and Compounds, 2014, 584, 180-184.	2.8	39
34	Multi-heterojunction photocatalysts based on WO3 nanorods: Structural design and optimization for enhanced photocatalytic activity under visible light. Chemical Engineering Journal, 2014, 237, 29-37.	6.6	63
35	Coexistence of an anatase/TiO2(B) heterojunction and an exposed (001) facet in TiO2 nanoribbon photocatalysts synthesized via a fluorine-free route and topotactic transformation. Nanoscale, 2014, 6, 5329.	2.8	46
36	Enhanced electrochromic properties of a TiO ₂ nanowire array via decoration with anatase nanoparticles. Journal of Materials Chemistry C, 2014, 2, 7891.	2.7	47

#	Article	IF	CITATIONS
37	Decorating hierarchical Bi2MoO6 microspheres with uniformly dispersed ultrafine Ag nanoparticles by an in situ reduction process for enhanced visible light-induced photocatalysis. Colloids and Surfaces A: Physicochemical and Engineering Aspects, 2013, 425, 99-107.	2.3	50
38	Rutile TiO2 nanowire array infiltrated with anatase nanoparticles as photoanode for dye-sensitized solar cells: enhanced cell performance via the rutile–anatase heterojunction. Journal of Materials Chemistry A, 2013, 1, 3309.	5.2	49
39	Heterostructured TiO2/WO3 porous microspheres: Preparation, characterization and photocatalytic properties. Catalysis Today, 2013, 201, 195-202.	2.2	118
40	Growth of single-crystalline rutile TiO2 nanowire array on titanate nanosheet film for dye-sensitized solar cells. Journal of Materials Chemistry, 2012, 22, 6389.	6.7	62
41	Tubular nanocomposite catalysts based on size-controlled and highly dispersed silver nanoparticles assembled on electrospun silicananotubes for catalytic reduction of 4-nitrophenol. Journal of Materials Chemistry, 2012, 22, 1387-1395.	6.7	251
42	Synthesis of Natural Cellulose-Templated TiO2/Ag Nanosponge Composites and Photocatalytic Properties. ACS Applied Materials & Interfaces, 2012, 4, 2781-2787.	4.0	144
43	Morphologically-tunable TiO2 nanorod film with high energy facets: green synthesis, growth mechanism and photocatalytic activity. Nanoscale, 2012, 4, 5023.	2.8	44
44	Simple route to self-assembled BiOCl networks photocatalyst from nanosheet with exposed (001) facet. Micro and Nano Letters, 2012, 7, 152.	0.6	35
45	Solar photocatalytic activities of porous Nb-doped TiO2 microspheres prepared by ultrasonic spray pyrolysis. Solid State Sciences, 2012, 14, 139-144.	1.5	77
46	Bi4Ti3O12 nanosheets/TiO2 submicron fibers heterostructures: in situ fabrication and high visible light photocatalytic activity. Journal of Materials Chemistry, 2011, 21, 6922.	6.7	113
47	Hydrothermal Growth of Layered Titanate Nanosheet Arrays on Titanium Foil and Their Topotactic Transformation to Heterostructured TiO ₂ Photocatalysts. Journal of Physical Chemistry C, 2011, 115, 22276-22285.	1.5	111
48	In situ assembly of well-dispersed gold nanoparticles on electrospun silica nanotubes for catalytic reduction of 4-nitrophenol. Chemical Communications, 2011, 47, 3906.	2.2	276
49	A Facile in Situ Hydrothermal Method to SrTiO ₃ /TiO ₂ Nanofiber Heterostructures with High Photocatalytic Activity. Langmuir, 2011, 27, 2946-2952.	1.6	269
50	Rutile TiO2 nanowires on anatase TiO2 nanofibers: A branched heterostructured photocatalysts via interface-assisted fabrication approach. Journal of Colloid and Interface Science, 2011, 363, 157-164.	5.0	50
51	One-Step Nonaqueous Synthesis of Pure Phase TiO ₂ Nanocrystals from TiCl ₄ in Butanol and Their Photocatalytic Properties. Journal of Nanomaterials, 2011, 2011, 1-6.	1.5	5
52	Three-dimensional hierarchical CeO2 nanowalls/TiO2 nanofibers heterostructure and its high photocatalytic performance. Journal of Sol-Gel Science and Technology, 2010, 55, 105-110.	1.1	28
53	Fabrication, structure, and enhanced photocatalytic properties of hierarchical CeO2 nanostructures/TiO2 nanofibers heterostructures. Materials Research Bulletin, 2010, 45, 1406-1412.	2.7	64
54	Electrospun Nanofibers of <i>p</i> -Type NiO/ <i>n</i> -Type ZnO Heterojunctions with Enhanced Photocatalytic Activity. ACS Applied Materials & Interfaces, 2010, 2, 2915-2923.	4.0	574

#	Article	IF	CITATIONS
55	Electrospun Nanofibers of ZnOâ^'SnO ₂ Heterojunction with High Photocatalytic Activity. Journal of Physical Chemistry C, 2010, 114, 7920-7925.	1.5	345
56	Polyacrylonitrile and Carbon Nanofibers with Controllable Nanoporous Structures by Electrospinning. Macromolecular Materials and Engineering, 2009, 294, 673-678.	1.7	119
57	Electrospinning preparation, characterization and photocatalytic properties of Bi2O3 nanofibers. Journal of Colloid and Interface Science, 2009, 333, 242-248.	5.0	183
58	ZnO Hollow Nanofibers: Fabrication from Facile Single Capillary Electrospinning and Applications in Gas Sensors. Journal of Physical Chemistry C, 2009, 113, 19397-19403.	1.5	189
59	SnO ₂ Nanostructures-TiO ₂ Nanofibers Heterostructures: Controlled Fabrication and High Photocatalytic Properties. Inorganic Chemistry, 2009, 48, 7261-7268.	1.9	311
60	Waterâ^'Dichloromethane Interface Controlled Synthesis of Hierarchical Rutile TiO ₂ Superstructures and Their Photocatalytic Properties. Inorganic Chemistry, 2009, 48, 1105-1113.	1.9	92
61	Photoluminescence properties of highly dispersed ZnO quantum dots in polyvinylpyrrolidone nanotubes prepared by a single capillary electrospinning. Journal of Chemical Physics, 2008, 129, 114708.	1.2	23
62	One-step sol–gel preparation and enhanced photocatalytic activity of porous polyoxometalate–tantalum pentoxide nanocomposites. Journal of Colloid and Interface Science, 2007, 308, 208-215.	5.0	36
63	A novel preparation of three-dimensionally ordered macroporous M/Ti (M=Zr or Ta) mixed oxide nanoparticles with enhanced photocatalytic activity. Journal of Colloid and Interface Science, 2006, 301, 236-247.	5.0	60
64	Three-dimensionally ordered macroporous Ti1â^'xTaxO2+x/2 (x=0.025, 0.05, and 0.075) nanoparticles: Preparation and enhanced photocatalytic activity. Materials Letters, 2006, 60, 2711-2714.	1.3	13